

Optical properties of a $\text{Nd}_{0.7}\text{Sr}_{0.3}\text{MnO}_3$ single crystal

H. J. Lee, J. H. Jung, Y. S. Lee, J. S. Ahn, and T. W. Noh

Department of Physics and Condensed Matter Research Institute, Seoul National University, Seoul 151-742, Korea

K. H. Kim

Department of Physics and Astronomy, Rutgers University, Piscataway, New Jersey 08855

S-W. Cheong

*Department of Physics and Astronomy, Rutgers University, Piscataway, New Jersey 08855
and Bell Laboratories, Lucent Technologies, Murray Hill, New Jersey 07974*

(Received 12 April 1999)

We investigated temperature-dependent optical conductivity spectra of a $\text{Nd}_{0.7}\text{Sr}_{0.3}\text{MnO}_3$ single crystal. We found that polishing and surface scattering effects on the $\text{Nd}_{0.7}\text{Sr}_{0.3}\text{MnO}_3$ crystal surfaces could significantly distort the optical responses, especially in the mid-infrared region. However, oxygen annealing and gold normalization processes seemed to remedy the distortions. We found that the spectral weight of $\text{Nd}_{0.7}\text{Sr}_{0.3}\text{MnO}_3$ in the metallic state might be composed of a Drude carrier term and a strong incoherent mid-infrared absorptions. The temperature dependence of the spectral weight suggests that the electron-lattice coupling should be important in optical properties of colossal magnetoresistance manganites.

[S0163-1829(99)03432-3]

I. INTRODUCTION

It has been well known that series of doped manganites with the chemical formula $R_{1-x}A_x\text{MnO}_3$ ($R = \text{La}$ or Nd , and $A = \text{Ca}$, Sr , or Ba) near $x \sim 0.3$ undergo paramagnetic insulator to ferromagnetic metal transitions and show colossal magnetoresistance (CMR) phenomena near the transitions. The coexistence of metallicity and ferromagnetism in manganites has been explained by the double-exchange (DE) interaction with a strong Hund coupling between e_g carrier and t_{2g} spins. However, it has been argued that some additional degrees of freedom, such as lattice,¹ orbital,² and disorder,³ should be included to explain the CMR quantitatively.

Optical measurements have been very useful to investigate the basic mechanisms of some insulator-metal transitions and associated electronic structure changes.⁴⁻⁷ There have been numerous optical investigations on manganites, however, the experimental data and their interpretations are varied. Especially, there are several different views on the spectral weights in the metallic states. Okimoto *et al.*⁴ measured optical responses of $(\text{La,Sr})\text{MnO}_3$ single crystals, and claimed that the corresponding Drude peaks are very weak and sharp. Similar behaviors were observed in $\text{La}_{0.7}\text{Ca}_{0.3}\text{MnO}_3$ polycrystalline samples by Kim, Jung, and Noh.⁸ However, Quijada *et al.*⁹ investigated $\sigma(\omega)$ of annealed $\text{Nd}_{0.7}\text{Sr}_{0.3}\text{MnO}_3$, $\text{La}_{0.7}\text{Ca}_{0.3}\text{MnO}_3$, and $\text{La}_{0.7}\text{Sr}_{0.3}\text{MnO}_3$ films on LaAlO_3 substrates, and observed broad and strong $\sigma(\omega)$ features at the low-frequency region. They attributed these features to Drude responses and coherent conduction. Boris *et al.*¹⁰ measured $\sigma(\omega)$ of a $\text{La}_{0.67}\text{Ca}_{0.33}\text{MnO}_3$ single crystal. At 78 K, its $\sigma(\omega)$ showed a very broad Drude-like behavior which was much stronger than those of polycrystalline samples. Takenaka *et al.*⁵ also measured $\sigma(\omega)$ of cleaved $(\text{La,Sr})\text{MnO}_3$ single crystals, and observed a Drude-like peak with a large spectral weight.

As one of the possible scenarios for such variations, Takenaka *et al.*⁵ reported that cleaved $(\text{La,Sr})\text{MnO}_3$ single crystals had optical spectra different from those of the polished crystals, and claimed that the small Drude weight in the polished samples observed by Okimoto *et al.*⁴ should be originated from damaged surfaces during the polishing process. The problem due to the sample preparation method is more serious for $\text{Nd}_{0.7}\text{Sr}_{0.3}\text{MnO}_3$ thin films. Kaplan *et al.*⁶ reported an optical response of a $\text{Nd}_{0.7}\text{Sr}_{0.3}\text{MnO}_3$ thin film. They could not observe the Drude-like peak even in the metallic region at low temperature. Later, Quijada *et al.*⁹ reported a Drude-like free carrier behavior for an oxygen-annealed $\text{Nd}_{0.7}\text{Sr}_{0.3}\text{MnO}_3$ film. Therefore, careful surface treatments and exact optical measurements are inevitable to get correct electrodynamic responses and to understand the basic mechanism of the CMR.

In this paper, we present optical conductivity spectra $\sigma(\omega)$ of a $\text{Nd}_{0.7}\text{Sr}_{0.3}\text{MnO}_3$ (NSMO) single crystal for annealed and polished surfaces. Although dc conductivity values of both surfaces were nearly the same, their $\sigma(\omega)$ were quite different. Using the oxygen annealing and gold normalization techniques, surface strain and surface scattering effects could be removed. Our experimental data suggested that the low-frequency spectral weight in the metallic states might be composed of a Drude part and a strong incoherent mid-infrared absorption. The temperature dependence of the spectral weight supports the conclusion that lattice effects are important in NSMO.

II. EXPERIMENT

The NSMO single crystal was prepared by floating zone methods. Details of crystal growth and characterizations were described elsewhere.¹¹ Just before optical measurements, the sample was polished up to $0.3 \mu\text{m}$ using dia-

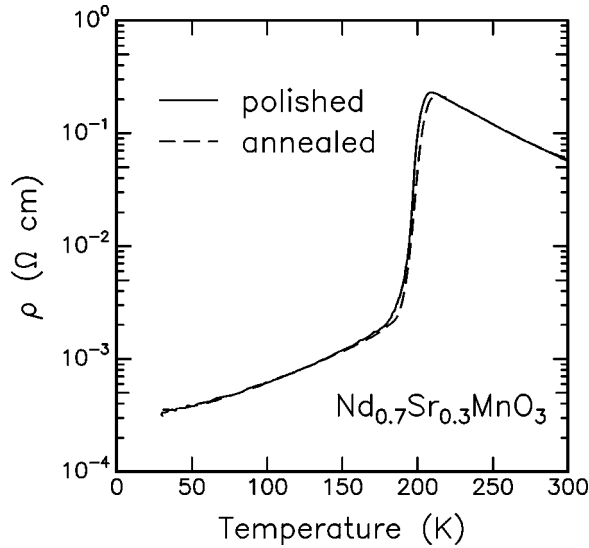


FIG. 1. $\rho(T)$ of the NSMO single crystal. The solid and the dashed lines represent the resistivity curves of polished and annealed NSMO, respectively.

mond pastes. After the polishing, we carefully annealed the sample again in an O_2 atmosphere at 1000°C for 1 h. Figure 1 shows values of temperature- $(T-)$ dependent dc resistivity $\rho(T)$ of our NSMO single crystal, which were measured by the conventional four-probe method. The solid and the dashed lines represent the $\rho(T)$ curves of the polished and the annealed NSMO, respectively. The $\rho(T)$ curves show a typical insulator-metal transition around 198 K. It seems that overall features of $\rho(T)$ for the polished and the annealed NSMO are nearly the same except for small deviations around T_C . Although such an annealing procedure does not change $\rho(T)$ significantly, it seems to be very important for optical properties of the NSMO sample. As demonstrated in the next section, optical properties of the NSMO crystal became drastically changed after the oxygen annealing.

Near normal incident reflectivity spectra, $R(\omega)$, were measured in a wide photon energy region of 5 meV–30 eV and at temperatures between 15 and 300 K. We used a conventional Fourier transform spectrophotometer between 5 meV and 0.8 eV. Above 0.6 eV, grating spectrometers were used. Especially above 6.0 eV, we used the synchrotron radiation from the normal incidence monochromator beam line at Pohang Light Source (PLS). T -dependent $R(\omega)$ below 6.5 eV were measured using a liquid-He-cooled cryostat. To subtract surface scattering effects from $R(\omega)$, we used the gold normalization technique:¹² a gold film was evaporated onto the sample surface just after spectra were taken. Then, the reflectivity of the gold-coated surface was measured and used for normalizing $R(\omega)$ of the NSMO sample.

Using the Kramers-Kronig (KK) analysis with the normalized $R(\omega)$, we obtained $\sigma(\omega)$. For this analysis, $R(\omega)$ in the low-frequency region were extrapolated with the Hagen-Rubens relation¹³ for metallic states and with constants for insulating states. To obtain accurate $\sigma(\omega)$ in the far-infrared region, we also compared $R(\omega)$ extrapolated using the Hagen-Rubens relation with those extrapolated using the Drude model, and we obtained nearly the same results in the far-infrared region. The T -dependent $R(\omega)$ spectra below 6.5 eV were smoothly connected with the reflectivity data ob-

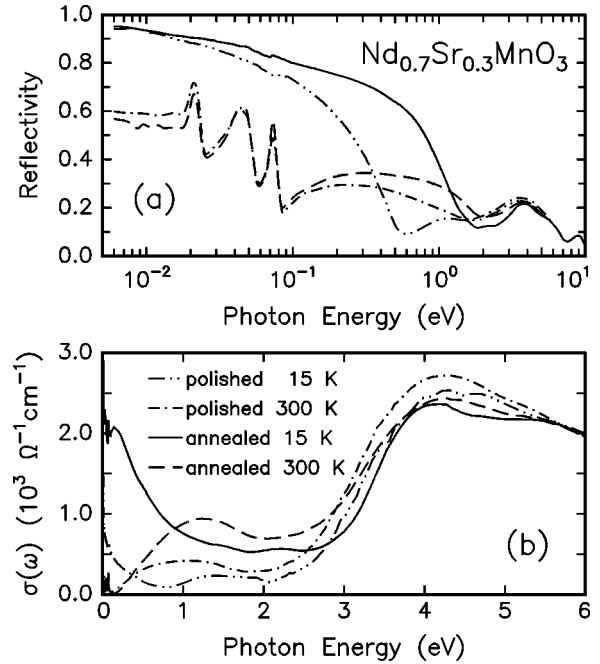


FIG. 2. (a) $R(\omega)$ and (b) $\sigma(\omega)$ for polished and annealed NSMO.

tained at room temperature from 6.0 to 30 eV, assuming that reflectivity in the high-energy region should be nearly temperature independent. For the frequency region above our measurements, the reflectivity at 30 eV was extended up to 40 eV and then ω^{-4} dependence was assumed. Using spectroscopic ellipsometry (SE), we obtained $\sigma(\omega)$ in the region of 1.5–5.0 eV without relying on the KK extrapolation. The $\sigma(\omega)$ obtained by the SE method were quite consistent with those obtained by the KK analysis. This fact suggests the validity of our gold normalization techniques and the extrapolations used in the KK analysis.

III. RESULTS AND DISCUSSION

A. Effects of oxygen annealing

Although the oxygen annealing process does not change $\rho(T)$ very much, it affects the optical responses of NSMO significantly. Figure 2(a) shows $R(\omega)$ for the polished and the annealed surfaces of the NSMO single crystal. (Note that both of these spectra were corrected by the gold normalization technique, so differences are mainly due to the oxygen annealing effects.) In the insulating region above T_C , the differences in $R(\omega)$ are not significant. However, in the metallic region below T_C , $R(\omega)$ for the polished surface are much lower in the frequency region from 2×10^{-2} to 1.5 eV. The dip in $R(\omega)$, the so-called “plasma edge,” for the polished surface appears around 0.6 eV, which is much lower than the observed dip around 2.0 eV for the annealed surface. The differences in the polished and the annealed surfaces can be clearly seen in $\sigma(\omega)$, which are displayed in Fig. 2(b). After the annealing, the spectral weight in the infrared region becomes considerably enhanced. Although Drude-like peaks at the far-infrared region can be observed at 15 K for both surfaces, $\sigma(\omega)$ of the polished surface has a smaller spectral weight.

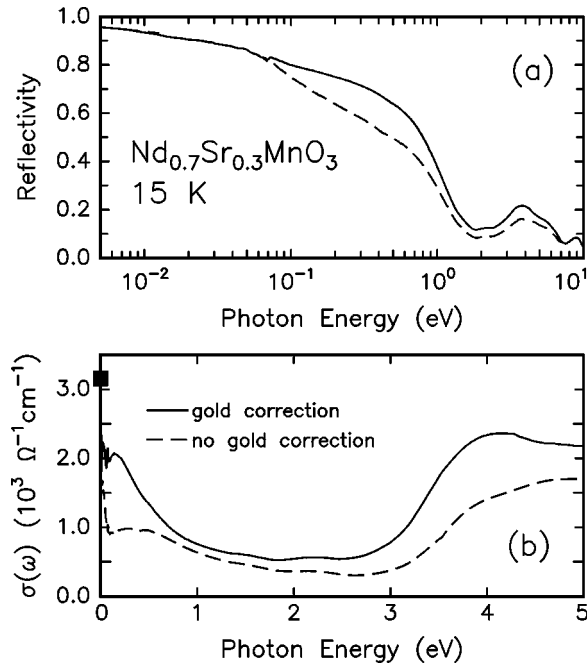


FIG. 3. (a) $R(\omega)$ and (b) $\sigma(\omega)$ for gold corrected and not corrected NSMO. In (b), the solid square denotes the value of dc conductivity.

Changes in the optical response due to the oxygen annealing were already noticed in NSMO thin films. Kaplan *et al.* reported that a NSMO film, whose resistivity peak temperature T_p was located around 180 K, had a strong mid-infrared peak and no Drude-like free carrier peak.⁶ Later, the same group reported that T_p of a NSMO film became about 230 K when it was annealed in an oxygen environment.⁹ They showed that the strength of the mid-infrared peak became considerably weakened and that the Drude-like free carrier behavior appeared in the oxygen-annealed NSMO film. We think that the optical response changes in the NSMO film were related to the dc resistivity changes reported by Xiong *et al.*¹⁴ They investigated the effects of oxygen annealing in NSMO films. With more annealing, their resistivity values became smaller and T_p moved to a higher temperature. They suggested that the annealing effects in the NSMO films could be explained by a change of oxygen content and a variation of mixed $\text{Mn}^{3+}/\text{Mn}^{4+}$ ratio.

Since $\rho(T)$ of our NSMO single crystal does not change by the annealing process, the optical response changes observed in Fig. 2 might not come from oxygen content changes. We think that the differences in optical spectra should be originated from damage due to the polishing process. Since the electron-phonon interactions are believed to be very strong in manganites, the stress applied during the polishing process could damage the surface region and deform optical responses significantly.

B. Effects of gold normalization

We also found that light scattering from the polished surface was quite severe in the NSMO sample. Figures 3(a) and 3(b) show $R(\omega)$ and $\sigma(\omega)$ of the oxygen annealed NSMO sample at 15 K, respectively. The dashed lines are results without any correction, and the solid lines are results after

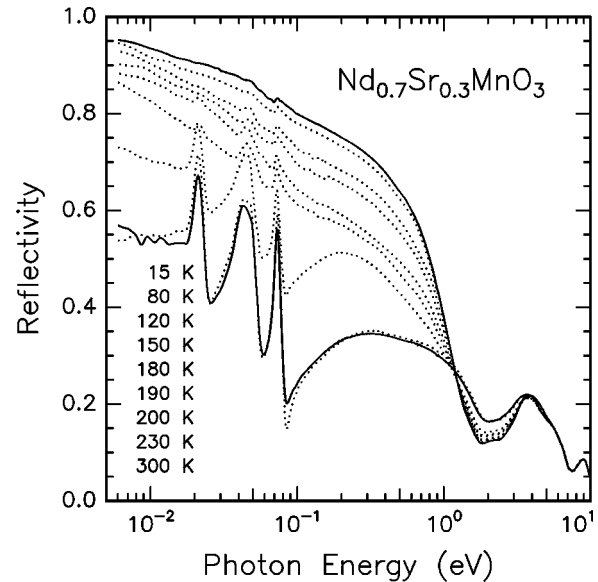


FIG. 4. T -dependent $R(\omega)$ of the annealed NSMO with gold correction.

the gold normalization. $R(\omega)$ in Fig. 3(a) show that the light scattering effects are not significant below 0.1 eV, but that they become very severe between mid-infrared and visible regions. The scattering loss effects become evident in $\sigma(\omega)$. Figure 3(b) shows that the spectral weight becomes reduced in most of the frequency region. Especially, the spectral change below 0.5 eV becomes quite large.

Recently, Takenaka *et al.*⁵ compared optical reflectivity spectra of $(\text{La,Sr})\text{MnO}_3$ cleavage surfaces with those of polished surfaces, and they showed that $\sigma(\omega)$ of the cleaved surface have a much more enhanced Drude weight. They claimed that the damage of the polished surface should result in a serious distortion in $\sigma(\omega)$. Since the optical spectra of their cleaved surface (i.e., Fig. 2 of Ref. 5) are very similar to our results after the oxygen annealing and the gold normalization processes, it can be suggested that the differences observed by Takenaka *et al.* were likely to be remedied by our experimental techniques.

C. Spectral weight in the insulating state

In Fig. 4, we show T -dependent $R(\omega)$ of the annealed NSMO single crystal from 5 meV to 10 eV. At 300 K, there are three sharp peaks originated from optic phonon modes in the far-infrared region. And, broad peaks above 0.1 eV come from the optical transitions between electronic levels. With decreasing T , the value of reflectivity approaches 1.0 in the dc limit (i.e., $\omega \rightarrow 0$) and the sharp phonon features become screened by the free carrier. Note that there is strong T dependence in $R(\omega)$ up to 5.0 eV. Similar behaviors were observed in other CMR manganites.^{9,15}

Figure 5 shows T -dependent $\sigma(\omega)$ of the annealed NSMO single crystal, which were obtained by the KK analysis. In the temperature region above T_C , we can see two interesting features: an optical gap near 0.18 eV, and broad peaks around 1.2 and 4.5 eV. As T decreases, a significant amount of spectral weight between 1.0 and 5.0 eV moves to a low-energy region. Above 5.0 eV, the spectral weight is nearly T independent. Due to the similarities in peak position and

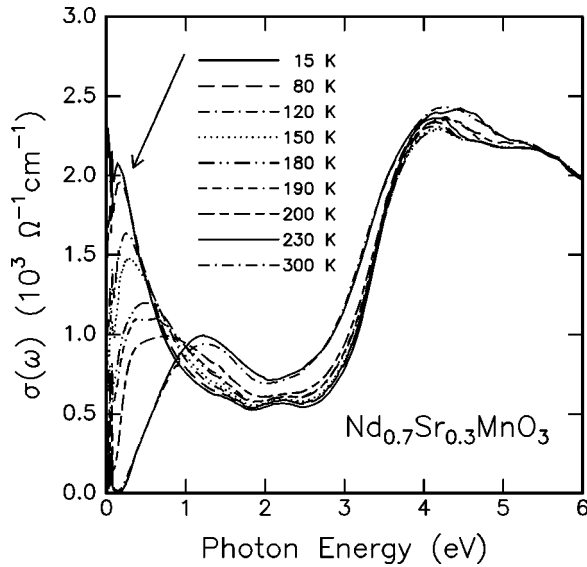


FIG. 5. T -dependent $\sigma(\omega)$ of the annealed NSMO with gold correction.

strength to those of charge-transfer transitions in the other manganites,^{15–17} the peak around 4.5 eV can be assigned to a charge-transfer transition between the O2p and the Mn e_g bands. The large spectral weight change between 2.0 and 5.0 eV can be interpreted in terms of an interband transition between the Hund rule split bands, i.e., $e_g^\uparrow(t_{2g}^\uparrow) \rightarrow e_g^\uparrow(t_{2g}^\downarrow)$ and $e_g^\downarrow(t_{2g}^\downarrow) \rightarrow e_g^\downarrow(t_{2g}^\uparrow)$, in the DE picture.^{18,19} (This notation indicates that the transitions occur between two e_g bands with the same spin but different t_{2g} spin background.) As T decreases below T_C , the spins of the t_{2g} electrons are pointing along one direction and the interband transition becomes weakened, which results in the decrease of the spectral weight.

Now, let us focus on the spectral weights in the insulating state. Although the peak near 1.2 eV appears to be one broad peak, we claim that it should be interpreted in terms of a two-peak structure:²⁰ one peak is located near 1.5 eV and the other is located below 1.0 eV. For most manganites with hole concentrations below 0.4, the 1.5 eV peak could not be seen clearly. However, there have been several reports which support the existence of the 1.5 eV peak.²¹ From doping-dependent conductivity studies on (La,Ca)MnO₃, Jung *et al.*¹⁶ showed that such a peak should exist. Machida, Moritome, and Nakamura²² also observed similar peaks in transmission spectra of (Nd_{0.25}Sm_{0.75})_{0.6}Sr_{0.4}MnO₃ and Sm_{0.6}Sr_{0.4}MnO₃ films. And, to explain optical spectra of Nd_{0.7}Sr_{0.3}MnO₃, La_{0.7}Ca_{0.3}MnO₃, and La_{0.7}Sr_{0.3}MnO₃ thin films, Quijada *et al.*⁹ assumed the existence of the 1.5 eV peak.

Moreover, if the broad peak around 1.2 eV is interpreted as one optical transition related to small polaron absorption, there will be some discrepancies between the optical data and other experimental data. For example, recent transport measurement shows that a small polaron activation energy should be about 0.15 eV,²³ which is smaller than 0.3 eV.²⁴ When we accept the double-peak structure, we can present a schematic diagram for the spectral weight in the insulating state, which is shown in Fig. 6(a). As shown in this diagram, there are four main peaks below 5.0 eV: (i) a small polaron

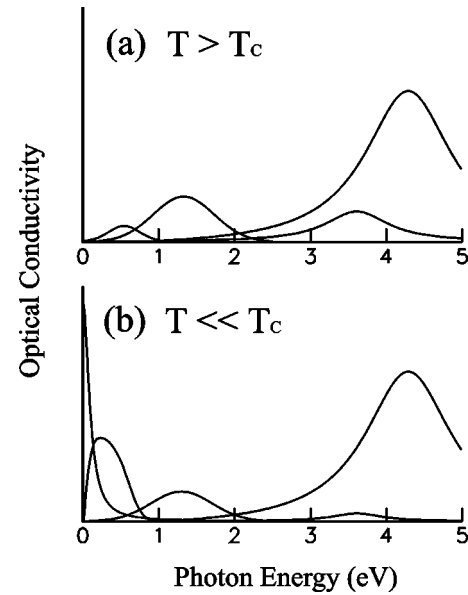


FIG. 6. Schematic diagrams for T -dependent $\sigma(\omega)$ of the NSMO for (a) $T > T_C$ and (b) $T \ll T_C$, respectively.

absorption peak below 1.0 eV, (ii) a peak centered around 1.5 eV, (iii) a broad peak centered around 3.5 eV, which is originated from interband transitions between the Hund rule split bands, and (iv) a peak due to charge-transfer transitions between the O 2p and the Mn e_g bands.

D. Spectral weight in the metallic state

Figure 7 shows detailed T -dependent $\sigma(\omega)$ below 2.0 eV. The solid square, triangle, and circle represent the measured dc conductivities of 15, 120, and 180 K, respectively. Above T_C , we can find three optic phonon modes. With cooling, the optic phonon modes become screened by the free carrier, but their signature can be observed even at 15 K. As T decreases below T_C , the spectral features above 0.8 eV decrease, and

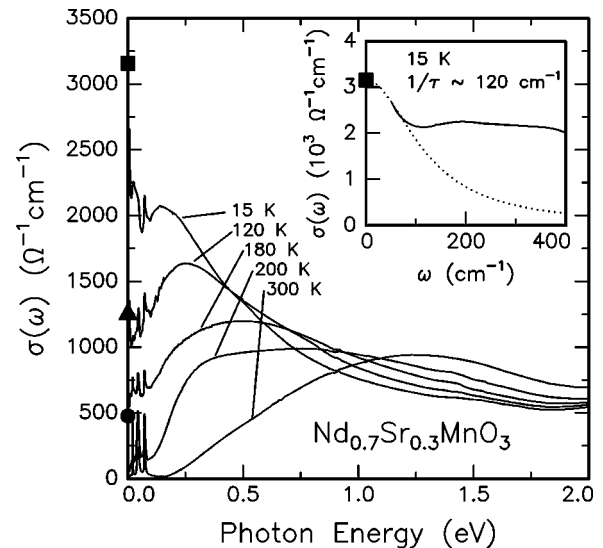


FIG. 7. Magnified $\sigma(\omega)$ of NSMO up to 2.0 eV. The solid square, triangle, and circle represent the dc conductivity values at 15, 120, and 180 K, respectively. In the inset, $\sigma(\omega)$ at 15 K are fitted with the simple Drude model.

those below 0.8 eV increase significantly. The increasing spectral weight below T_C seems to form an asymmetric band, whose peak position moves down with decreasing temperature. Even at 15 K, $\sigma(\omega)$ seem to make a downturn around 0.1 eV, and the corresponding dc conductivity is higher by about $1000 \Omega^{-1} \text{ cm}^{-1}$ than $\sigma(\omega=0.1 \text{ eV})$. It should be noted that our $\sigma(\omega)$ data at 15 K, displayed in Fig. 7, are similar to the low-temperature spectral responses observed by Quijada *et al.*⁹ and Boris *et al.*¹⁰

One important question which we should address at this point is whether we should interpret the low-frequency broad absorption feature at 15 K as a single-component Drude peak. There are three important experimental facts which we should notice. First, our experimental data showed the downturn of optical conductivity around 0.1 eV at $T \ll T_C$. The $\text{La}_{0.67}\text{Ca}_{0.33}\text{MnO}_3$ single-crystal data of Boris *et al.*¹⁰ showed the same behavior, and the thin film data of Quijada *et al.*⁹ showed similar trends, although such behaviors were neglected by the authors since the downturn regions were close to the low-frequency infrared cutoff of LaAlO_3 substrates. Second, the spectral weight changes of all the reported experiments, including the NSMO single-crystal case displayed in Fig. 7, cannot be described by a decrease of one spectral component at a fixed frequency and an increase of a single Drude component near the zero frequency. Rather, they can be reasonably described by a continual evolution of an asymmetric peak whose position moves down as the sample changes from the insulating state to the metallic state. A similar trend was observed for the room temperature data of the cleaved $(\text{La,Sr})\text{MnO}_3$ single crystals, investigated by Takenaka *et al.*⁵ As Sr doping increased and the sample became more metallic, a spectral weight increased in the low-frequency region, which could be described by a continual movement of an asymmetric peak. Third, some optical data cannot provide reasonable values for electrodynamic quantities, when a single-component Drude peak is assumed. For example, the single-crystalline $\text{La}_{0.67}\text{Ca}_{0.33}\text{MnO}_3$ data at 78 K indicate mean free path $l=3.9\text{--}5.2 \text{ \AA}$, which is comparable to the lattice constant a . This value is rather too small for metallic conduction.²⁵ On the other hand, assuming the two-component response for $\text{La}_{0.7}\text{Ca}_{0.3}\text{MnO}_3$ polycrystals, Kim, Jung, and Noh⁸ reported that $l \sim 25 \text{ \AA}$ at 15 K and that l becomes about 4.2 \AA near the metal-insulator transition temperature.

Therefore, we think that the low-frequency response should be interpreted in terms of two components, i.e., a coherent narrow Drude peak and an incoherent mid-infrared absorption band. Figure 6(b) shows a diagram of $\sigma(\omega)$ for $T \ll T_C$, which takes account of the two-component contributions. Another feature of the diagram is that the peak due to the charge-transfer transition is nearly T independent. In addition, as temperature decreases below T_C , the transition between the Hund rule split bands becomes weakened and the spectral weight below 1.0 eV increases significantly.

As displayed in Fig. 7, the incoherent mid-infrared absorption band is quite asymmetric and the Drude weight starts just below the characteristic phonon mode frequency. These optical features are quite consistent with coherent and incoherent absorptions of a large polaron, predicted by Emin.²⁶ From these observations, it can be argued that a crossover from small to large polaron states accompanies the

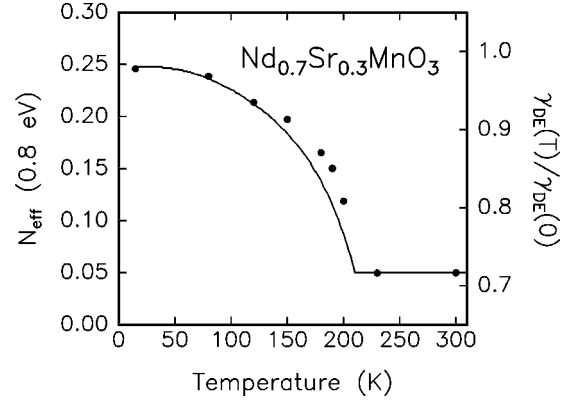


FIG. 8. T -dependent N_{eff} (0.8 eV) of the NSMO single crystal. The solid line refers to the behavior of $\gamma_{\text{DE}}(T)/\gamma_{\text{DE}}(0)$.

insulator-metal transition in NSMO. Such a crossover from the small to the large polaron was also observed by other experiments, including Raman scattering²⁷ and pulsed pair density function (PDF) measurements.²⁸ In this polaron crossover scenario, the strong oxygen annealing dependence of the optical responses in the metallic states might be explained. Just after the polishing, the surface region should be damaged quite significantly, which blocks the motion of incoherent polaron motion. However, after the annealing, such stress-induced damages could be repaired. More detailed investigations are needed to clarify this scenario.

E. Temperature dependence of low-energy spectral weight

To get a further understanding of the low-energy spectral weight, we evaluated the effective number of carriers, $N_{\text{eff}}(\omega_C)$, below a cutoff frequency ω_C :

$$N_{\text{eff}}(\omega_C) = \frac{2m_e}{\pi e^2 N} \int_0^{\omega_C} \sigma(\omega') d\omega', \quad (1)$$

where m_e is a free electron mass and N represents the number of Mn atoms per unit volume. For actual estimation, the value of ω_C was chosen to be 0.8 eV, since the low-frequency spectral weight below $\sim 0.8 \text{ eV}$ increases as T decreases below T_C , as displayed in Fig. 7.

Figure 8 shows the T dependence of N_{eff} (0.8 eV). Above T_C , N_{eff} is nearly independent of T . As T decreases, N_{eff} shows an increasing behavior. In the simple DE picture, the spectral weight of the Drude carriers should be proportional to $(1+M^2)/2$, where M is the magnetization. However, measured magnetization data show a very sharp increase near T_C , so a quantitative agreement between N_{eff} and $(1+M^2)/2$ could not be obtained. Recently, Kim *et al.* investigated optical properties of $(\text{La,Pr})_{0.7}\text{Ca}_{0.3}\text{MnO}_3$,²⁹ and found that all of the N_{eff}/T_C data for various values of Pr concentration can be scaled with $\gamma_{\text{DE}}(T)$, which represents the temperature-dependent DE bandwidth due to spin ordering within the DE model predicted by Kubo and Ohata.³⁰ To explain this scaling behavior, they adopted the theoretical results³¹ based on a Hamiltonian including the DE interaction and Jahn-Teller (JT) electron-phonon coupling terms. They showed that $N_{\text{eff}} \approx t\xi\gamma_{\text{DE}}(T)$, where ξ is the polaronic band narrowing term. The solid line in Fig. 8 represents the predicted behavior of $\gamma_{\text{DE}}(T)/\gamma_{\text{DE}}(0)$, which agrees quite

well with the evaluated values of N_{eff} (0.8 eV). This agreement suggested that both the DE interaction and the JT electron-phonon coupling play important roles in NSMO.

F. Electrodynamic quantities

One of the important issues in barely conducting materials is to determine electrodynamic quantities, such as scattering rate $1/\tau$, carrier density n , and effective mass m^* . The mean free path l and dc conductivity σ can be written in terms of the electrodynamic quantities:

$$l = \tau \hbar (3 \pi^2 n)^{1/3} / m^*, \quad (2)$$

and

$$\sigma = ne^2 \tau / m^*. \quad (3)$$

Assuming hole carrier conduction (i.e., $n=0.3$), l at 15 K was estimated to be about 13 Å. [When we assumed electron carrier conduction (i.e., $n=0.7$), l should be about 7 Å.] As shown in the inset of Fig. 7, we fitted the free carrier absorption with the simple Drude model and found that $1/\tau \sim 120 \pm 20 \text{ cm}^{-1}$ provided a reasonable fit to our low-frequency data. Using this value of $1/\tau$, we found that $m^*/m_e \sim 21 \pm 3$.

Values of m^* could be estimated using other experimental techniques, such as specific heat measurements. Conduction carriers provide a T -linear term, whose coefficient γ can be written as $\pi^2 k_B^2 N(E_F)/3$, where k_B and $N(E_F)$ are the Boltzmann constant and density of states at the Fermi energy, respectively. In the free electron model, the corresponding linear coefficient γ_0 can be written as $(4\pi^3 m_e k_B^2 V / 3h^2)(3n/\pi)^{1/3}$, where h is Planck's constant. Therefore, γ/γ_0 should be the same as m^*/m_e . From specific heat measurements of $\text{Nd}_{0.67}\text{Sr}_{0.33}\text{MnO}_3$, Gordon *et al.*³² reported the values of $\gamma(T=0)$ as 25 mJ/K² mol. (Note that γ_0 was estimated to be around 0.9 mJ/K² mol.) However, they claimed that the value of γ/γ_0 , i.e., 26, was too large for the conduction carrier contribution, and that the coupling between Nd and Mn spins might enhance the value of γ .

Note that our estimated value of m^*/m_e for NSMO is larger than those of other manganites. From specific heat measurements, Hamilton *et al.*³³ found that γ/γ_0 was around 5 for $\text{La}_{0.67}\text{Ba}_{0.33}\text{MnO}_3$ and around 8 for $\text{La}_{0.8}\text{Ca}_{0.2}\text{MnO}_3$. And, from optical measurements, Kim, Jung, and Noh⁸ reported $m^*/m_e \sim 13$ for $\text{La}_{0.7}\text{Ca}_{0.3}\text{MnO}_3$. In the DE model, T_C should be proportional to an effective transfer integral t_{eff} for an electron hopping between Mn ions. And, in the tight binding calculation, $N(E_F)$ is inversely proportional to t_{eff} . Since γ is proportional to $N(E_F)$, γ should also be inversely proportional to t_{eff} . From the fact that T_C of NSMO is quite smaller than those of $\text{La}_{0.7}\text{Ca}_{0.3}\text{MnO}_3$ and $\text{La}_{0.67}\text{Ba}_{0.33}\text{MnO}_3$, the large value of m^* in NSMO seems to be reasonable. This also supports the validity of our analysis for the NSMO metallic state in terms of a small Drude weight and a strong incoherent peak.

IV. CONCLUSION

We investigated the temperature-dependent optical conductivity spectra of a $\text{Nd}_{0.7}\text{Sr}_{0.3}\text{MnO}_3$ single crystal. We found that the polishing process could damage the surface region of the crystal and deform the optical spectra quite significantly. Using the oxygen annealing process and the gold normalization technique, such damage due to the polishing process seems to be recovered. Based on optical conductivity spectra, we provided schematic diagrams for spectral weight distributions in the metallic and the insulating regions. We found that the optical response in the metallic region should be interpreted in terms of a Drude part and a strong incoherent mid-infrared absorption.

ACKNOWLEDGMENTS

We thank H. K. Lee, N. J. Hur, Dr. E. J. Choi, Dr. H. C. Lee, and Dr. Y. Chung for useful discussion and helpful experiments. We acknowledge the financial support by the Ministry of Education through Grant No. BSRI-98-2416, by the Korea Science and Engineering Foundation through Grant No. 971-0207-024-2, and through RCDAMP of Pusan National University. Experiments at PLS were supported in part by MOST and POSCO.

¹A. J. Millis, B. I. Shraiman, and R. Mueller, Phys. Rev. Lett. **77**, 175 (1996).

²S. Ishihara, M. Yamanaka, and N. Nagaosa, Phys. Rev. B **56**, 686 (1997).

³L. Sheng, D. Y. Xing, D. N. Sheng, and C. S. Ting, Phys. Rev. B **56**, R7053 (1997).

⁴Y. Okimoto, T. Katsufuji, T. Ishikawa, A. Urushibara, T. Arima, and Y. Tokura, Phys. Rev. Lett. **75**, 109 (1995); Y. Okimoto, T. Katsufuji, T. Ishikawa, T. Arima, and Y. Tokura, Phys. Rev. B **55**, 4206 (1997).

⁵K. Takenaka, K. Iida, Y. Sawaki, S. Sugai, Y. Moritomo, and A. Nakamura, cond-mat/9810035 (unpublished).

⁶S. G. Kaplan, M. Quijada, H. D. Drew, D. B. Tanner, G. C. Xiong, R. Ramesh, C. Kwon, and T. Venkatesan, Phys. Rev. Lett. **77**, 2081 (1996).

⁷K. H. Kim, J. Y. Gu, H. S. Choi, G. W. Park, and T. W. Noh,

Phys. Rev. Lett. **77**, 1877 (1996).

⁸K. H. Kim, J. H. Jung, and T. W. Noh, Phys. Rev. Lett. **81**, 1517 (1998).

⁹M. Quijada, J. Černe, J. R. Simpson, H. D. Drew, K. H. Ahn, A. J. Millis, R. Shreekala, R. Ramesh, M. Rajeswari, and T. Venkatesan, Phys. Rev. B **58**, 16 093 (1998).

¹⁰A. V. Boris, N. N. Kovaleva, A. V. Bazhenov, P. J. M. van Bentum, Th. Rasing, S-W. Cheong, A. V. Samoilov, and N.-C. Yeh, Phys. Rev. B **59**, R697 (1999).

¹¹J. A. Fernandez-Baca, P. Dai, H. Y. Hwang, C. Kloc, and S-W. Cheong, Phys. Rev. Lett. **80**, 4012 (1998).

¹²J. H. Jung, K. H. Kim, D. J. Eom, T. W. Noh, E. J. Choi, Jaejun Yu, Y. S. Kwon, and Y. Chung, Phys. Rev. B **55**, 15 489 (1997).

¹³K. H. Kim, J. Y. Gu, H. S. Choi, D. J. Eom, J. H. Jung, and T. W. Noh, Phys. Rev. B **55**, 4023 (1997).

¹⁴G. C. Xiong, Q. Li, H. L. Ju, R. L. Greene, and T. Venkatesan,

- Appl. Phys. Lett. **66**, 1689 (1995).
- ¹⁵J. H. Jung, K. H. Kim, H. J. Lee, J. S. Ahn, N. J. Hur, T. W. Noh, M. S. Kim, and J.-G. Park, Phys. Rev. B **59**, 3793 (1999).
- ¹⁶J. H. Jung, K. H. Kim, T. W. Noh, E. J. Choi, and Jaejun Yu, Phys. Rev. B **57**, R11 043 (1998).
- ¹⁷H. L. Liu, S. L. Cooper, and S-W. Cheong, Phys. Rev. Lett. **81**, 4684 (1998).
- ¹⁸N. Furukawa, Y. Moritomo, K. Hirota, and Y. Endoh, cond-mat/9808076 (unpublished).
- ¹⁹Y. Moritomo, A. Machida, K. Matsuda, M. Ichida, and A. Nakamura, Phys. Rev. B **56**, 5088 (1997).
- ²⁰There is a theory paper supporting the two-peak structure. S. Yunoki, A. Moreo, and E. Dagotto, Phys. Rev. Lett. **81**, 5612 (1998).
- ²¹There are still some debates on the origin of the 1.5 eV peak. Quijada *et al.* (Ref. 9) assigned it to an interatomic transition between the Mn^{3+} levels split due to the Jahn-Teller distortion. Machida and co-workers (Ref. 19) attributed it to an optical transition related to the JT clusters. Jung *et al.* (Ref. 16) assigned it to an intra-atomic transition between JT split Mn^{3+} levels. More systematic studies are required to get a better understanding of the origin of the 1.5 eV peak.
- ²²A. Machida, Y. Moritomo, and A. Nakamura, Phys. Rev. B **58**, 12 540 (1998); **58**, R4281 (1998).
- ²³Guo-meng Zhao (private communication).
- ²⁴It is known that the energy of a small polaron motion measured by optical techniques is about four times larger than the activation energy measured by transport measurements. If the 1.2 eV peak is the small polaron absorption peak, the activation energy determined by the transport measurements should be 0.3 eV. Refer to P. A. Cox, *Transition Metal Oxides* (Clarendon Press, Oxford, 1992).
- ²⁵According to the Ioffe-Regal criteria, $l \sim a$ near metal-insulator transition. For the metallic state, $l \gg a$. Refer to *The Metallic and Nonmetallic States of Matter*, edited by P. P. Edwards and C. N. R. Rao (Taylor & Francis, London, 1985), Chap. 2.
- ²⁶D. Emin, Phys. Rev. B **48**, 13 691 (1993).
- ²⁷S. Yoon, H. L. Liu, G. Schollerer, S. L. Cooper, P. D. Han, D. A. Payne, S-W. Cheong, and Z. Fisk, Phys. Rev. B **58**, 2795 (1998).
- ²⁸D. Louca, T. Egami, E. L. Brosha, H. Röder, and A. R. Bishop, Phys. Rev. B **56**, R8475 (1997).
- ²⁹K. H. Kim, J. H. Jung, D. J. Eom, T. W. Noh, Jaejun Yu, and E. J. Choi, Phys. Rev. Lett. **81**, 4983 (1998).
- ³⁰K. Kubo and N. Ohata, J. Phys. Soc. Jpn. **33**, 21 (1972).
- ³¹H. Röder, J. Zhang, and A. R. Bishop, Phys. Rev. Lett. **76**, 1356 (1996).
- ³²J. E. Gordon, R. A. Fisher, Y. X. Jia, N. E. Phillips, S. F. Reklis, D. A. Wright, and A. Zettl, Phys. Rev. B **59**, 127 (1999).
- ³³J. J. Hamilton, E. L. Keatly, H. L. Ju, A. K. Raychaudhuri, V. N. Smolyaninova, and R. L. Greene, Phys. Rev. B **54**, 14 926 (1996).